

Original

Assessment of Hepatocellular Carcinoma Ablation Margins Using Fused Pre-ablation Hepatobiliary Phase and Post-ablation Unenhanced T1-weighted Images

Nobuyuki TAKEYAMA*¹⁾, Naruki MIZOBUCHI²⁾, Masashi SAKAKI³⁾,
Yu SHIMOZUMA³⁾, Atsushi KAJIWARA³⁾, Manabu UCHIKOSHI³⁾,
Jiro MUNESHIKA²⁾, Syojiro UOZUMI³⁾, Yoshimitsu OHGIYA²⁾
and Toshi HASHIMOTO¹⁾

Abstract : This study retrospectively investigated the value of fusing a pre-ablation hepatobiliary phase (HBP) series and post-ablation unenhanced T1-weighted images (T1WIs) to evaluate the treatment effectiveness of radiofrequency ablation for hepatocellular carcinoma (HCC). Predictors of local tumor progression (LTP) were also identified. Our study comprised 47 patients with 88 HCCs (>2 years follow up) who underwent pre-ablation gadoxetate disodium-enhanced magnetic resonance imaging and post-ablation T1-weighted imaging. For the new assessment, pre-ablation HBP series and post-ablation T1WIs were fused using a rigid registration and manual correlation, and the ablation margin appearance was classified as ablation margin (+), ablation margin zero, ablation margin (-), or indeterminate (index tumor was invisible) based on the post-ablation T1WIs and fusion images. The minimal ablation margin was measured and clinical factors were investigated to identify other risk factors for LTP, which was observed in 14 tumors. The mean minimal ablation margin was 1.9 mm, excluding 5 indeterminate nodules without LTP, and 8 ablation margin-zero HCCs with LTP, with multivariate logistic regression analysis showing that the likelihood of ablation margin+ was inversely proportional to tumor size. The independent risk factors for LTP were not identified, but the cumulative LTP rates (0% at 1, 2, and 3 years) in 41 ablation margin+ nodules were significantly lower ($P=0.005$) than those (8.8%, 17.6%, and 17.6% at 1, 2, and 3 years, respectively) in 34 ablation margin-zero nodules. In conclusion, fusion images might show an early therapeutic response of the ablated tumors in the majority of HCC cases.

Key words : radiofrequency ablation, fusion image, T1-weighted image, hepatobiliary phase

¹⁾ Department of Radiology, Showa University Fujigaoka Hospital, 1-30 Fujigaoka, Aoba-ku, Yokohama 227-8501, Japan.

²⁾ Department of Radiology, Division of Radiology, Showa University School of Medicine.

³⁾ Department of Medicine, Division of Gastroenterology, Showa University School of Medicine.

* To whom corresponding should be addressed.

Introduction

Radiofrequency (RF) ablation is widely used as a minimally invasive therapy for early-stage hepatocellular carcinoma (HCC)^{1,2}; however, incomplete treatment can leave a residual tumor and induce local tumor progression (LTP)³⁻⁵. Among various risk factors identified for LTP, achieving a sufficient ablation margin is crucial as an independent factor for both progression-free survival and overall survival^{1,2}.

Contrast-enhanced computed tomography (CT) has been used to assess the therapeutic response after RF ablation whereby pre- and post-ablation CT images are compared in a side-by-side manner; however, this approach can be inaccurate because pre- and post-ablation liver images frequently differ⁵⁻⁷. Moreover, the ablation-induced hyperemia surrounding the ablation zone may mimic residual tumor^{8,9}. To overcome these limitations, the fusion of pre- and post-ablation images on CT⁴⁻⁷ or post-ablation magnetic resonance imaging (MRI)¹⁰⁻¹⁷ has been developed.

For the post-ablation MRI, unenhanced T1-weighted images (T1WIs) can distinguish the index tumor from the ablation margin on the same image. In one such example, Onishi *et al*¹³ reported that a central hypo- or hyper-intense tumor covered by a hyperintense ablation margin with the marginal hypointense band corresponded pathologically with the index tumor, coagulation necrosis, and sinusoidal congestion with fibrosis. Further, Khankan *et al*¹⁴ reported that >95% of index tumors could be discriminated from the ablation margin no more than 2 days after RF ablation. In contrast, Kim *et al*¹⁵ and Koda *et al*¹⁶ described that 19–36% of index tumors could not be detected 7 hours after ablation, while Takeyama *et al*¹⁷ demonstrated that 56% of such tumors were invisible 24 hours after ablation. Furthermore, a tumor-liver contrast ratio during pre-ablation hepatobiliary phase (HBP) on gadoxetate disodium-enhanced MRI (EOB-MRI) was 0.8 ± 0.6 and the absolute value of tumor-liver contrast ratio on post-ablation T1WIs was 5^{16,17}. These findings thus suggested that signal intensity differences between index tumors and ablation zones provide obvious contrast among them under the post-processing feasibility of MR-MR fusion^{7-9,18-20} and that fusion imaging could overcome the limitation of post-ablation T1WIs because post-ablation unenhanced MRI examinations have been routinely acquired no more than 2 days after RF ablation for HCCs at our institution.

The purpose of this study was to clarify the clinical utility of fusion images from a pre-ablation HBP series and post-ablation T1WIs obtained no more than 2 days after the procedure, compared with post-ablation T1WIs. Additionally, factors to indicate an adequate ablation margin and factors to predict LTP were evaluated on fusion imaging.

Methods

Patients

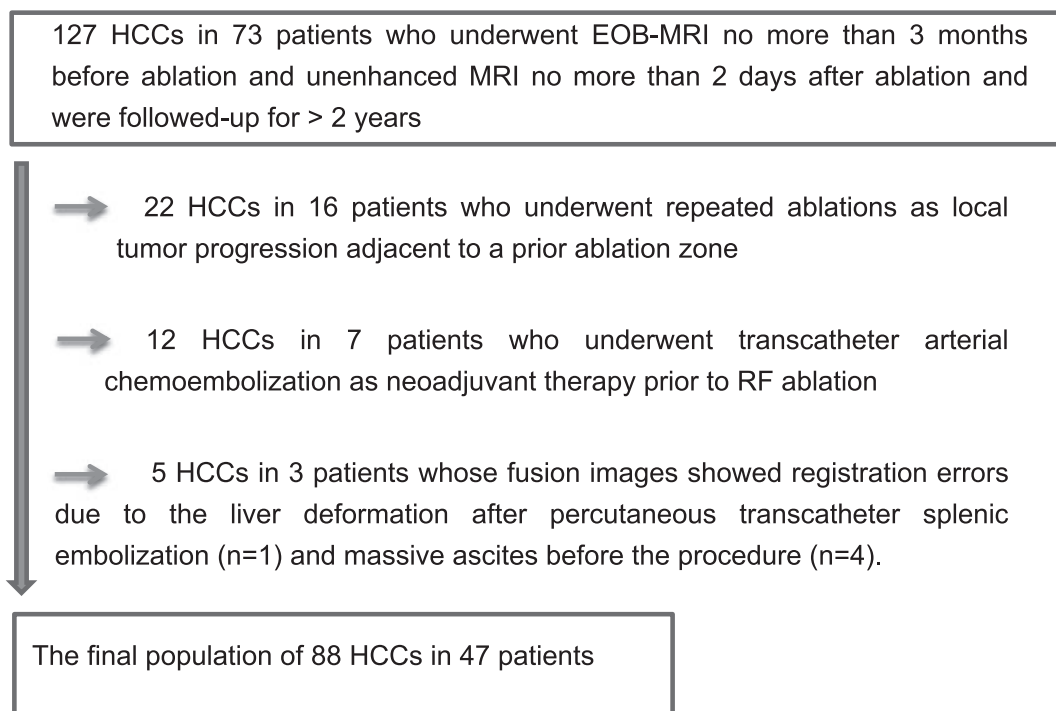
The School of Medicine, Showa University Ethics Committee approved this retrospective study (permission number 2,356), and the informed consent requirement was waived for all patients.

In our institution, MR examinations have always been acquired routinely no more than 2 days

after the procedure in patients with HCC. Thus, we searched our radiology reports database from December 2011 to March 2017 for patients who met the following criteria: “RF ablation for HCC”, “EOB-MRI no more than 3 months before ablation and unenhanced MRI no more than 2 days after ablation” and “patients who were followed-up for > 2 years²¹⁾”, resulting in 127 HCCs from 73 patients.

We excluded the following cases: 22 HCCs in 16 patients due to repeated ablations as LTP adjacent to a prior ablation zone, 12 HCCs in 7 patients who underwent transcatheter arterial chemoembolization (TACE) as neoadjuvant therapy prior to RF ablation, and 5 HCCs in 3 patients whose fusion could not be achieved by registration errors due to the severe deformation after percutaneous transcatheter splenic embolization (n=1) and massive ascites before the procedure (n=4). Finally, 88 HCCs in 47 patients were enrolled in this study (Fig. 1).

HCC was diagnosed as a tumor showing hypervascularity on the arterial phase with washout on the portal venous phase²²⁾, or a tumor showing hypervascularity on the arterial phase with hypointensity during HBP if it was difficult to evaluate washout²³⁾. The tumor diameter was measured using the arterial phase, portal venous phases, and HBP. Clinical stage was determined using the Child-Pugh classification, and treatment stages were accepted in Child-Pugh classes A and B. Clinical data were collected about underlying chronic liver disease (alcohol,



RF : radiofrequency, EOB-MRI : gadoxetate disodium-enhanced MRI, HCC : hepatocellular carcinoma

Fig. 1. Flow chart of inclusion and exclusion criteria in this study

hepatitis B, hepatitis C, non-alcoholic steatohepatitis, and primary biliary cirrhosis), past therapies (RF ablation, TACE, or hepatectomy in other segments), and number of lesions (single or multiple). Serum alpha-fetoprotein (AFP) was measured before RF ablation²⁴, and tumor location was determined by the Couinaud segmental anatomical classification into three patterns: 1) subcapsular and subdiaphragmatic, 2) within 3 mm of the first to third branches of the portal vein, hepatic vein, or inferior vena cava, and 3) others (Table 1).

RF Ablation Procedure

Four experienced hepatologists performed ultrasound-guided RF ablation using a 17-gauge cooled-tip electrode with a 2- or 3-cm-long exposed metallic tip (Cool-Tip Radiofrequency System, Covidien, Boulder, CO). The electrode was repositioned to create an effective ablation margin surrounding the tumor. In cases of multifocal tumor, several lesions were ablated in the same session. When the tumor was located in the hepatic dome, an artificial pleural effusion technique was used to improve tumor visibility. A routine track ablation was done for all tumors.

MRI protocol

Pre-ablation EOB-MRI was acquired no more than 3 months (mean 35.3 ± 24.6 days, ranging from 1 to 90 days) before the procedure. Pre-ablation MRI examinations included T2-weighted, diffusion-weighted, unenhanced T1-weighted, and dynamic contrast-enhanced images using either a 1.5-T system (Avanto or Essenza, Siemens Healthcare) or a 3-T system (Trio, Siemens Healthcare). The dynamic study involved administration of Gd-EOB-DTPA (Primovist, Bayer

Table 1. Characteristics of 88 hepatocellular carcinomas (HCCs) in 47 patients

Characteristics	Value
Age (year) : mean \pm SD (range)	73.8 \pm 10.4 (40-90)
Gender: male / female	36 / 11
Follow-up (month) : mean \pm SD (range)	45.2 \pm 15.7 (24-71)
Tumor size (mm) : mean \pm SD (range)	12.4 \pm 5.6 (5-30)
Child-Pugh score: A / B / C	78 / 10 / 0
Etiology: Alcoholism / HBV / HCV / NASH / PBC	11 / 2 / 25 / 8 / 1
Past history: RFA / TACE / Hepatectomy / none	14 / 18 / 8 / 48
Tumor multiplicity: simple / multiple	41 / 47
AFP (ng/ml)	73.5 \pm 150.9 (1-569)
Tumor location:	
Abutting vessels / Subcapsular or diaphragmatic / no	21 / 40 / 27
Caudate lobe / Left lobe / Right anterior segment / Right posterior segment	1 / 28 / 39 / 20

HBV : hepatitis B virus, HCV : hepatitis C virus, NASH : non-alcoholic steatohepatitis, PBC : primary biliary cirrhosis, AIH : autoimmune hepatitis, RFA : radiofrequency ablation, TACE : transcatheter arterial chemoembolization, AFP : alpha-fetoprotein

Healthcare, Osaka, Japan) at 0.025 mmol/kg of body weight followed by a 20-ml saline flush at a rate of 2 ml/s using a power injector. Arterial phase, portal venous phase, late phase, and HBP images were obtained at 20 seconds, 60 seconds, 120 seconds, and 20 minutes, respectively, and the contrast-enhanced T1WI and HBP sequences represented volumetric interpolated breath-hold examination (VIBE) sequences with fat saturation using the following parameters: TR range, 2.91–4.97 msec; TE range, 1.13–1.83 msec; and flip angle, 9–15°. Post-ablation unenhanced MRI included T2-weighted, diffusion-weighted, and 3D-Dixon water images, using the following parameters: TR range (3.29–7.22 msec), TE range (1.13–2.38 msec), and flip angle (12–15°). All images were scanned in the axial plane. The range of section thicknesses was 3.5–5.0 mm and the matrix range was from 224–281 to 300–350 pixels. The averaged section thickness was 3.9 ± 0.4 mm during pre-ablation HBP and 4.0 ± 0.3 mm on post-ablation T1WIs. The average gap between pre- and post-ablation MRI was 0.35 ± 0.3 mm, including gaps of 0 mm in 36 lesions, 0.5 mm in 48, 1 mm in 2, and 1.5 mm in 2 lesions.

Follow-up after the procedure

The post-ablation HBP series were acquired no more than 2 days (mean 1.04 days) after ablation. If hepatologists interpreted that a tumor was not covered sufficiently by the ablation zone on post-ablation MRI, RF ablation was repeated the next day after MRI to encompass the tumor sufficiently, and 6 HCCs in 5 patients who required additional ablation underwent unenhanced MRI examinations no more than 2 days after the procedure were included in this study. In all patients, EOB-MRI was repeated every 2–4 months for 2 years, and multiphasic contrast-enhanced CT or EOB-MRI was repeated every 6 months thereafter. When LTP was detected during the follow-up period, RF ablation or TACE was used.

Fusion imaging

An image analysis system (Volume Analyzer Synapse VINCENT, version 5.1, Fujifilm Medical Systems, Tokyo, Japan) used a rigid registration method to create fusion images, according to the Couinaud sub-segmental anatomical location around the target tumor^{7,20}.

First, the “Fusion” application was clicked to superimpose pre-ablation HBP series onto post-ablation T1WIs. The registration program started with axial, coronal, sagittal, and 3D views.

Second, automatic registration was conducted to align pre- and post-ablation MR images and finally, manual registration was performed at the sub-segmental anatomical location around the target tumor by selecting the adjacent portal vein or hepatic venous branch. The bifurcation point of each vessel was assigned as a landmark, with 10 points *selected* on axial views, 5 points on coronal views, and 5 points on sagittal views.

Third, target nodules and the ablation zone were colored. The “lung low attenuation area” color was selected among 7 colors as lower images and the “Rad blue-2” color was chosen from 21 colors as upper images. The index tumor, ablation margin, and peripheral rim appeared as a pink or pale nodule, a lilac colored area, and an ultramarine or purple rim, respectively.

The mean time to create one registration image was approximately 15 minutes.

Qualitative analysis

Two radiologists with 4 and 24 years of experience in abdominal imaging independently interpreted the post-ablation T1WIs and fusion images using a workstation. In cases of discrepancies between the two readers, a final decision was made via consensus through reassessment with a third radiologist who had 11 years of experience in abdominal imaging. These clinicians knew the diagnosis of HCC and information about tumor location and size, but not the final results as to whether LTP occurred during the follow-up period. Post-processing to scroll windowing, gradation adjustment, or magnification was freely used.

First, they scored the registration error of the portal and hepatic vein branches in the targeted area using the following three criteria: good, no (0 mm) vascular misregistration; fair, minimal (<2 mm) in less than 4 vessels; and poor, minimal (<2 mm) in more than 5 vessels, or severe (>3 mm) in more than 1 vessel^{8, 18-20}.

Second, they assessed the ablation margin. Pre-ablation T1-weighted, arterial phase, late phase, and HBP images were initially observed, and then post-ablation T1WIs and fusion images were reviewed. The ablation margin was graded as follows; visible [ablation margin (+), ablation margin zero, and ablation margin (-)] and indeterminate (Fig. 2). An indeterminate was judged when a central lesion could not be discriminated from the ablation zone^{12, 15}. The ablation margin plus [ablation margin (+)] demonstrated that an ablation zone completely covered a tumor. The ablation margin zero represented a partially discontinuous ablation margin without tumor protrusion, while a minus margin score [ablation margin (-)] indicated a tumor protruding partially from the ablation margin. Post-ablation T1WIs revealed a visible ablation margin to be a central hypo- or hyperintense tumor encompassed by a hyperintense broad middle zone with a hypointense marginal band. Fusion imaging revealed a visible ablation margin to be a central pink or pale tumor surrounded by a broad iliac-colored middle zone with an ultramarine rim (Fig. 3).

The size and shape of the visible target lesions on post-ablation T1WIs and fusion images were similar or slightly collapsed compared with the pre-ablation HBP series.

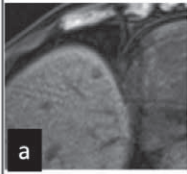
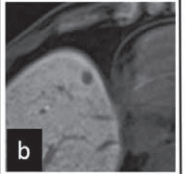
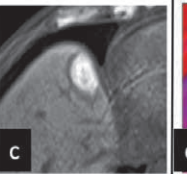
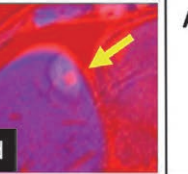

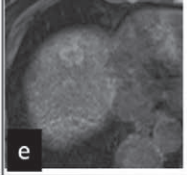
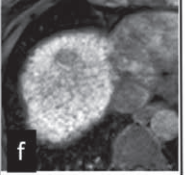
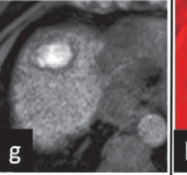
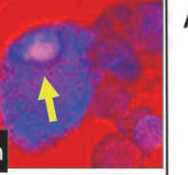

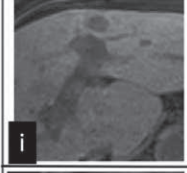

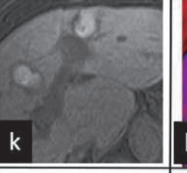
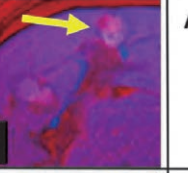

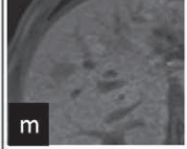
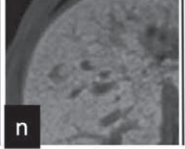
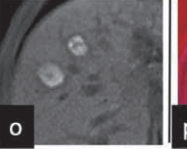
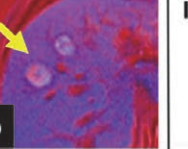

Quantitative analysis

The minimum ablation margin was measured in the ablation margin (+) nodules on fusion imaging as the shortest distance between the tumor boundaries and ablation margin peripheries using axial, coronal, and sagittal imaging (Fig. 4).

Statistical analysis

Inter-observer agreement on the ablation margin grading of post-ablation T1WIs and fusion images in 88 HCCs were analyzed using the Cohen k coefficient. The k values were interpreted as poor for k less than 0.20; fair, k of 0.21-0.40; moderate, k of 0.40-0.60; good, k of 0.61-0.80; and very good, k of 0.81-1.00.

The numbers and percentages of patients evaluated for the ablation margin grading [ablation margin (+), ablation margin zero, ablation margin (-), and indeterminate] on post-ablation

Pre-ablation T1W image	Pre-ablation HBP image	Post-ablation T1W image	Fusion image	Assessment of the ablation margin status
				Ablation margin (+) 
				Ablation margin (0) 
				Ablation margin (-) 
				Indeterminate 

AM : ablation margin, HCC : hepatocellular carcinoma

Fig. 2. Representative assessments of ablation margin status

Schemata of the ablation margin (AM) status were categorized into the following four types: ablation margin (+), ablation margin (0), ablation margin (-), and indeterminate. The first schema showed successful ablation and subsequent involution of the ablation zone. At pre-ablation MR imaging, the T1-weighted image (a) and the hepatobiliary phase series (b) demonstrated a 7-mm hypointense tumor in S4 of the liver. After radiofrequency ablation, the index tumor was invisible within the ablation zone on post-ablation T1-weighted imaging (c), while the fusion image (d) showed a central pink tumor encompassed by a broad lilac-colored ablation margin (arrow). The minimum ablation margin in this case was 1.3 mm, and was assessed as ablation margin (+). The second schema also shows successful ablation and subsequent involution of the ablation zone, with an 18-mm tumor graded as hyperintense on pre-ablation T1-weighted imaging (e) and hypointense on the hepatobiliary phase (f) in S8 of the liver. After radiofrequency ablation, the index tumor was invisible within the ablation zone by post-ablation T1-weighted imaging (g), while the fusion image (h) shows that the lilac-colored ablation margin was partially discontinuous, without protrusion of a central pink tumor beyond the border of the ablative margin. The ablation margin status was therefore assessed as ablation margin (0). The next schema shows incomplete ablation, with a nodular remnant of tumor tissue at the margin of the ablation zone. A 15-mm tumor was identified as hyperintense on the pre-ablation T1-weighted image (i) and hypointense on the hepatobiliary phase (j) in S3 of the liver. After radiofrequency ablation, the index tumor was invisible within the ablation on the post-ablation T1-weighted image (k), and the fusion image (l) demonstrated a subcapsular crescentic pink residual tumor (arrow) against the lilac-colored ablation zone. The status was assessed as ablation margin (-). The final schema shows successful ablation and subsequent involution of the ablation zone. A 12-mm tumor was identified as hypointense on pre-ablation T1-weighted imaging (m) and on the hepatobiliary phase (n) in S8 of the liver. After radiofrequency ablation, the index tumor was invisible within the ablation on the post-ablation T1-weighted image (o). The fusion image (p) also demonstrates a heterogeneous pink tumor (arrow) against the lilac-colored ablation zone. The ablation margin status was assessed as indeterminate.

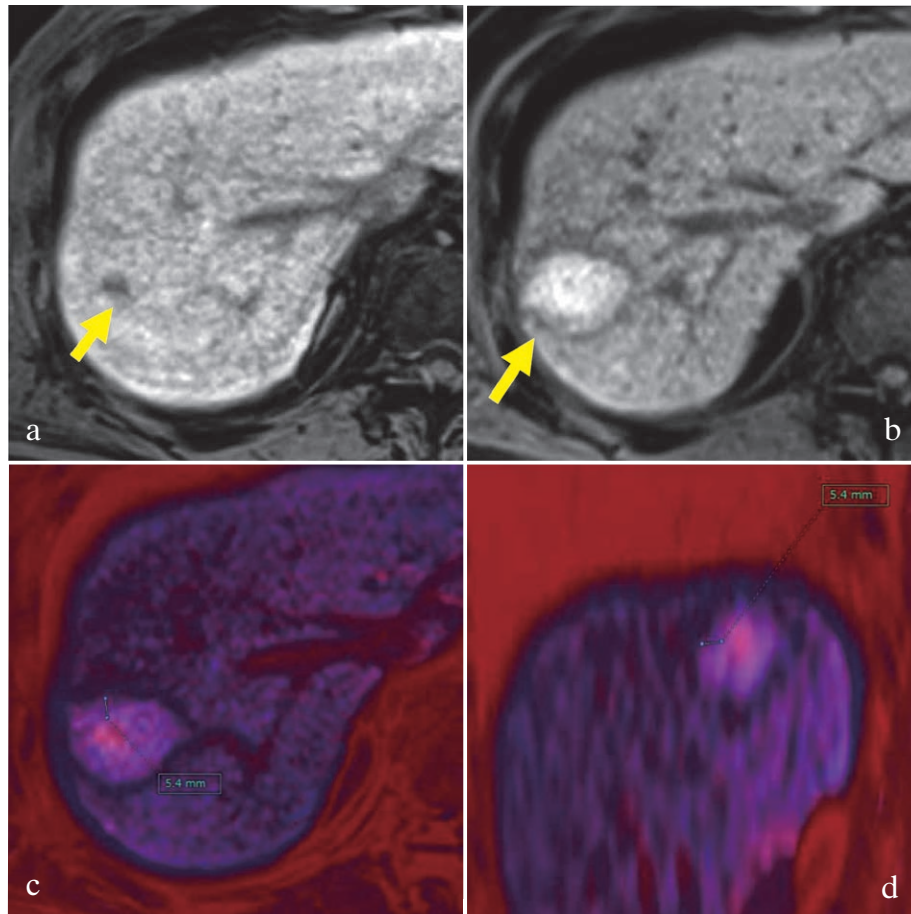


Fig. 3. A 73-year-old man underwent radiofrequency ablation of a 9-mm hepatocellular carcinoma in S8 of the liver
 (a) The pre-ablation hepatobiliary phase sequence showed a hypointense nodule (arrow) (b), and post-ablation T1-weighted imaging revealed a hyperintense ablation zone with the hypointense rim. The target nodule was invisible and the ablation margin grading was indeterminate (arrow). Fusion images of the axial (c) and coronal (d) views showed that a central pink tumor was sufficiently circumscribed by a broad, lilac-colored middle zone in all views. The ablation margin was scored as ablation margin (+), and the minimum ablation margin was 5.4 mm in the sagittal and coronal views. There was no local tumor progression at 36 months after the procedure.

HBP and fusion images were compared using the Chi-squared test.

Categorical variables were analyzed using the Chi-squared test as the univariate analysis to compare the baseline characteristics between ablation margin (+) and ablation margin zero HCCs on fusion imaging. A logistic regression model was used for multivariate analyses of independent factors for the ablation margin (+) on fusion imaging. The cumulative LTP rate was calculated using the Kaplan-Meier method and the log-rank test. Multivariate analysis of independent factors for LTP was analyzed by the Cox proportional hazard model.

Statistical analysis was performed using SPSS version 26 (IBM SPSS, Chicago, IL). Candidate

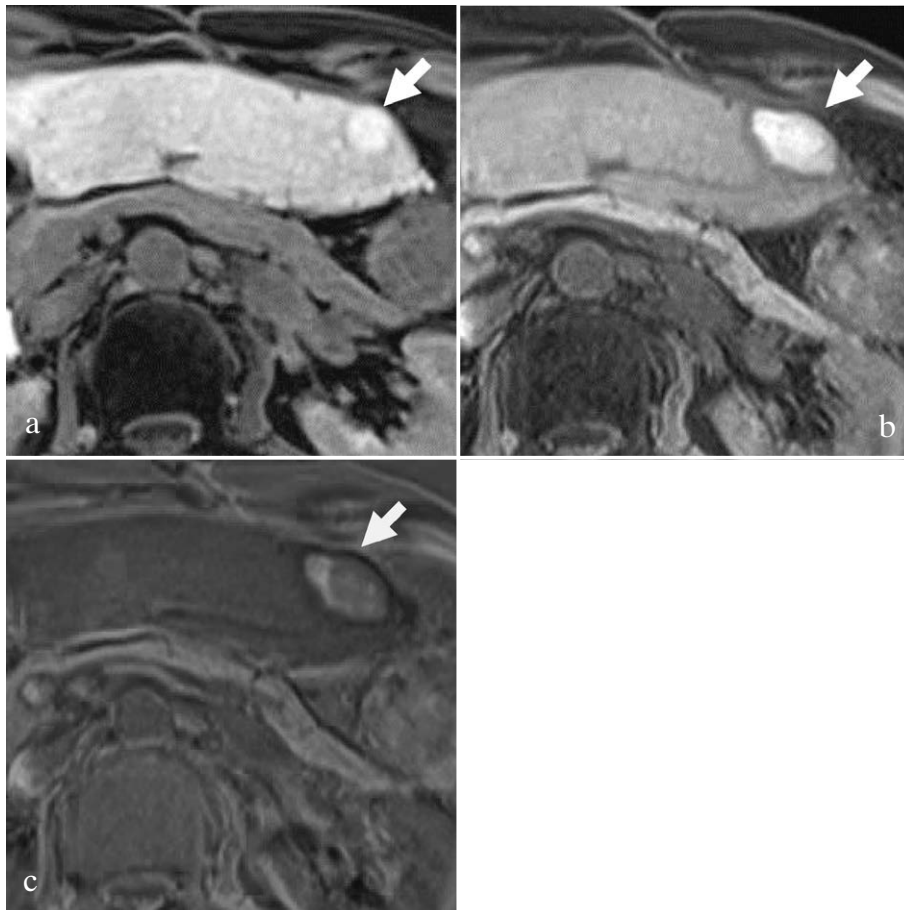


Fig. 4. A 63-year-old man underwent radiofrequency ablation for a 16-mm HCC in S3 of the liver

(a) The hepatobiliary phase sequence revealed the hyperintense nodule (arrow), which showed hypervascularity on the arterial phase and washout on the portal venous phase. (b) Post-ablation T1-weighted imaging revealed a heterogeneous hyperintensity of the ablation zone with a hypointense rim. The target nodule was not visualized and the ablation margin grading was indeterminate. Fusion images in the axial (c) view show that the pale tumor did not protrude beyond the border of the lilac ablative margin (arrow) contacting an ultramarine band (ablation margin zero). There was no local tumor progression at 36 months after the procedure.

variables with $P < 0.20$ in the univariate analyses were included in the multivariate logistic regression. Probability values < 0.05 were considered significant.

Results

Assessment of ablation margin grading on fusion imaging

Evaluation of the registration error for 88 HCCs on fusion images was good in 62 cases and fair in 26; no images rated as poor. The inter-observer agreement level between two radiologists for registration errors in the 88 HCCs on fusion images was good ($k=0.634$). An artificial pleural effusion was used in 17 (19.3%) of the 88 HCCs; however, no lesions showed

registration errors.

Assessment of the ablation margin for the 88 HCC nodules revealed 83 visible (94.3%) ablation margins and 5 indeterminate (5.7%) ablation margins. These five indeterminate nodules showed iso-hypointensity on the pre-ablation HBP series, with central pink or pale nodules that could not be distinguished from the lilac ablation zones (Fig. 2).

The mean time to LTP was 12.8 ± 5.2 months, ranging from 4 to 20 months. Of the 88 HC nodules, 14 (15.9%) showed LTP, including 8 of 8 (100%) ablation margin (-) nodules and 6 of 34 (17.6%) ablation margin zero nodules, of which three were re-treated by additional RF ablation on the following day after MRI showing the inadequate ablation margin. The remaining 74 lesions (84.1%) had no LTP, including the 5 indeterminate, 28 ablation margin (0), and 41 ablation margin (+) nodules.

Comparing the assessment of ablation margin grading on fusion imaging with post-ablation T1WIs

The ablation margin grading of 88 HCCs on post-ablation T1WIs revealed 8 ablation margin (+), 13 ablation margin zero, 2 ablation margin (-), and 65 indeterminate ablation margin, while the grading on fusion images showed 41 ablation margin (+), 34 ablation margin zero, 8 ablation margin (-) and 5 indeterminate ablation margin nodules.

The inter-observer agreement levels between two radiologists for the ablation margin grading were moderate on both post-ablation T1WIs ($k=0.513$) and fusion imaging ($k=0.500$); 23 (26.1%) of 88 nodules were identified on post-ablation T1WIs, and 83 of 88 (94.3%) nodules were visible on fusion images.

T1WIs (8, 13, 2, and 65) thus significantly outperformed fusion images (41, 34, 8, and 5) in the ablation margin (+), ablation margin zero, ablation margin (-), and indeterminate gradings (Table 2). In 41 ablation margin (+) nodules, the minimum ablation margin between the index tumor and the periphery of the ablation margin was 2.0 ± 1.0 mm, ranging from 1.0 mm to 5.6 mm.

Comparison between ablation margin (+) and ablation margin zero nodules on fusion imaging

Baseline characteristics of the 41 ablation margin (+) and 34 ablation margin zero HCCs were then compared, excluding 8 ablation margin (-) and 5 indeterminate HCCs. A multivariate logistic regression analysis showed that the likelihood of ablation margin (+) was inversely proportional to tumor size (Table 3).

The cumulative LTP rates (0%, 0%, and 0% at 1, 2, and 3 years, respectively) in 41 ablation margin (+) nodules were significantly lower than those (8.8%, 17.6%, and 17.6% at 1, 2, and 3 years, respectively) in 34 ablation margin zero nodules (Fig. 5a). The cumulative LTP rates (1.9%, 1.9%, and 1.9% at 1, 2, and 3 years, respectively) in 54 nodules sized < 15 mm were significantly lower than those (9.5%, 23.8%, and 23.8% at 1, 2, and 3 years, respectively) in 21 nodules sized ≥ 15 mm (Fig. 5b). No independent factors for LTP were identified using the multivariate Cox proportional hazards model (Table 4).

Table 2. Comparison of the numbers in the ablation margin grades between post-ablation unenhanced T1-weighted images and fused images

		Fusion images				
	Ablation margin grades	Ablation margin (+)	Ablation margin (0)	Ablation margin (-)	Indeterminate	Total
Unenhanced	Ablation margin (+)	8	0	0	0	8
T1-weighted	Ablation margin (0)	3	10	0	0	13
imaging	Ablation margin (-)	0	0	2	0	2
	Indeterminate	30	24	6	5	65
Total		41	34	8	5	88

Table 3. Baseline characteristics of tumors with ablation margin (+) nodules and ablation margin (0), and multivariate analysis of factors associated with ablation margin (+) on fusion images

	AM (+) n = 41	AM (0) n = 34	Univariate*	B	Multivariate** standard error (B)	P value
Age: ≥ 70 y or < 70 y	15 / 26	16 / 18	0.480			
Gender: male / female	29 / 12	20 / 14	0.334			
Etiology: HCV / not	19 / 22	18 / 16	0.646			
Child-Pugh score: A / not	39 / 2	30 / 4	0.401			
Past therapy: yes / no	17 / 24	15 / 19	1.000			
Tumor size: ≥ 15 mm / < 15 mm	7 / 34	14 / 20	0.037	1.217	3.377	0.027
Tumor multiplicity: simple / multiple	18 / 23	17 / 17	0.647			
AFP (≥ 50 ng/ml / < 50 ng/ml)	10 / 31	9 / 25	1.000			
Tumor location						
Continuous vessel / not	12 / 29	5 / 29	0.134	-0.864	0.422	0.160
Subcapsular or non-subcapsular	18 / 23	15 / 19	1.000			
S4 / 8 or no	3 / 38	3 / 31	1.000			

* : Chi-square test, ** : Multivariate logistic regression analysis, HCV : hepatitis C virus, AFP : α -fetoprotein

Discussion

Post-ablation T1WIs are rated highly by many researchers for indicating treatment efficacy after RF ablation. At the same time, using only T1WIs is considered challenging because an imaging hallmark of successful treatment is lack of enhancement in the index tumor using dynamic phases on CT and MRI^{24, 25}. Therefore, fusion images of the pre-ablation HBP series and post-ablation T1WIs could have the possibility to overcome limitations.

Post-ablation unenhanced MRI examinations have some benefits, including no peripheral hyperemia around the ablation zone, no radiation exposure, and no use of contrast agent. On post-ablation T1WIs, many index tumors are no longer visible, and in this study, 73.9% of nodules were scored as indeterminate, which represents a higher rate than previous reports^{12, 17}.

Table 4. Univariate and multivariate analysis of local tumor progression after RF ablation in 41 ablation margin (+) and 34 ablation margin zero nodules

Characteristics	Total (n=75)	LTP (n=6)	No LTP (n=69)	Univariate* P value	Multivariate** P value
Age: ≥ 70 y or < 70 y	44 / 31	4 / 2	40 / 29	0.684	
Gender: male / female	49 / 26	2 / 4	47 / 22	0.087	0.356
Etiology: HCV / none	32 / 43	2 / 4	30 / 39	0.612	
Child-Pugh score: A / B	69 / 6	6 / 0	63 / 6	0.461	
Past therapy: yes / no	32 / 43	2 / 4	30 / 39	0.612	
Tumor size: ≥ 15 mm / < 15 mm	21 / 54	5 / 1	16 / 53	0.002	0.087
Tumor multiplicity: simple / multiple	35 / 40	4 / 2	31 / 38	0.316	
AFP (≥ 50 ng/ml / < 50 ng/ml)	19 / 56	2 / 4	17 / 52	0.595	
Tumor location					
Continuous vessel / not	17 / 58	1 / 5	16 / 53	0.705	
Subcapsular / non-subcapsular	33 / 42	3 / 3	30 / 39	0.777	
S4 / 8 or not	6 / 69	1 / 5	5 / 64	0.435	
Ablation margin grade: ablation margin (+) / ablation margin (0)	41 / 34	0 / 6	41 / 28	0.005	0.954

HCV : hepatitis C, LTP : local tumor progression, AFP : α -fetoprotein

* : log-rank test, ** : Cox proportional hazards test

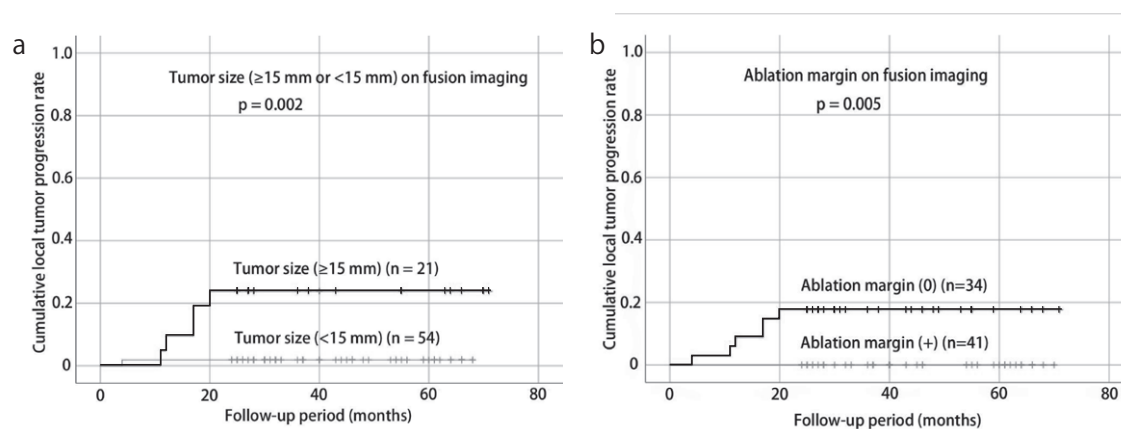


Fig. 5.

The Kaplan-Meier curves calculated according to the tumor size (≥ 15 mm or < 15 mm) (a), and the ablation margin grading (b) on fusion imaging. Cumulative local recurrence rates in nodules on fusion imaging of the pre-ablation hepatobiliary phase series and post-ablation T1-weighted images showed cumulative local recurrence rates in all 75 hepatocellular carcinomas according to tumor size (a) and classification of ablative margins (b) as follows: ablation margin zero (red line), with no residuals, but with sites of no margin; ablation margin (+) (blue line), which had an ablative margin with complete ablation. The log-rank test was used.

We speculated that several factors might affect tumor visibility, including elapsed time after the procedure, tumor size, tumor signal intensity, ablation procedure time, background liver function, and section thickness. Interestingly, 94.3% of visible target lesions within the ablation zone on fusion imaging was superior to that of previous MRI studies^{12,17}. Consequently, it is expected

that fusion imaging could solve this discrepancy on reports.

Previous methods to use fusion images, involving CT-CT fusion and MR-MR fusion, used a rigid registration method^{7,18-20}. This study used a segmentation technique that did not require manual tracing of the tumor, whereby two images were overlapped when the upper images were superimposed onto lower images. Consequently, tumors could be clearly discriminated from the ablation zone because their size and shape were similar compared with the tumor on pre-ablation HBP images. Although the acquisition parameters including TR, TE, FOV, and section thickness between pre- and post-ablation examinations differed, registration errors were not identified.

To date, various risk factors related to LTP after RF ablation have been identified^{1,2}. LTP is typically caused by the ablation margin status²⁵, the minimum ablation margin, incomplete placement of the probe, a heat sink effect owing to the proximity of large vessel, or large tumor size²⁶. Of these, the ablation margin has been recognized as the most significant risk factor for LTP because it can be measured quantitatively on fusion imaging of pre- and post-ablation images. The mean ablation margin was 1.9 mm in this study, noting that these data were different from a safety margin of 3–5 mm because we measured the area of the coagulation necrosis surrounding the index tumor without measuring the peripheral inflammation and granulation tissue²⁻⁷.

The LTP rate in the ablation margin (+) nodules showed 0% at 2 and 3 years because 41 of 41 (100%) ablation margin (+) nodules were treated without LTP. Although the Cox proportional hazard model analysis demonstrated that neither tumor size nor ablation margin status were independent predictors for LTP in this study, accurate evaluation of the ablation margin status in the early period after the procedure can lead to additional ablations^{12,24,26-28}. Because tumor size is also a significant factor for the ablation margin (+) on fusion imaging, ensuring that an adequate ablation margin is obtained should be considered when evaluating post-ablation images for larger nodules. Moreover, indeterminate ablation margin nodules should be carefully observed during the follow-up period or should be evaluated again.

This study had several limitations. First, reddish hepatic vessels appeared as a pink color similar to the index tumors, and careful interpretation is thus needed to discriminate these two structures from each other when in close proximity. Second, it was retrospective, and nodules that showed LTP were biased since 3 of 6 (50%) ablation margin zero nodules re-treated by the additional RF ablation were included. Further, similar studies are thus needed in a prospective study. Third, 3D-VIBE images had lower spatial resolution compared with previous reports¹⁷⁻²⁵. Spatial resolution should be improved using thin section thickness in future work.

Conclusions

In this study, fusion images comprising those from the pre-ablation HBP sequence and post-ablation T1WIs were superior to post-ablation T1WIs alone in assessing RF ablation, and such a method could produce an earlier assessment to predict LTP.

Conflict of interest disclosure

The authors declare no conflicts of interest regarding this study.

References

- 1) Kim YS, Lim HK, Rhim H, *et al*. Ten-year outcomes of percutaneous radiofrequency ablation as first-line therapy of early hepatocellular carcinoma: analysis of prognostic factors. *J Hepatol*. 2013;**58**:89–97.
- 2) Peng ZW, Zhang YJ, Chen MS, *et al*. Risk factors of survival after percutaneous radiology ablation of hepatocellular carcinoma. *Surg Oncol*. 2007;**17**:23–31.
- 3) Nakazawa T, Kokubu S, Shibuya A, *et al*. Radiofrequency ablation of hepatocellular carcinoma: correlation between local tumor progression after ablation and ablative margin. *AJR*. 2007;**188**:480–488.
- 4) Kim YS, Lee WJ, Rhim H, *et al*. The minimal ablative margin of radiofrequency ablation of hepatocellular carcinoma (>2 and <5 cm) needed to prevent local tumor progression: 3D quantitative assessment. *AJR*. 2010;**195**:758–765.
- 5) Shin S, Lee JM, Kim KY, *et al*. Postablation assessment using follow-up registration of CT images before and after Radiofrequency Ablation (RFA): prospective evaluation of midterm therapeutic results of RFA for Hepatocellular Carcinoma. *AJR*. 2014;**203**:70–77.
- 6) Makino Y, Imai Y, Igura T, *et al*. Utility of computed tomography fusion imaging for the evaluation of the ablative margin of radiofrequency ablation for hepatocellular carcinoma and the correlation to local tumor progression. *Hepatol Res*. 2013;**43**:950–958.
- 7) Kim KW, Lee JM, Klotz E, *et al*. Safety margin assessment after radiofrequency ablation of the liver using registration of preprocedure and postprocedure CT images. *AJR*. 2011;**196**:W565–W572.
- 8) Park MH, Rhim H, Kim YS, *et al*. Spectrum of CT findings after radiofrequency ablation of hepatic tumors. *Radiographics*. 2008;**28**:379–390.
- 9) Kim YS, Rhim H, Lim HK, *et al*. Coagulation necrosis induced by radiofrequency ablation in the liver: histopathologic and radiologic review of usual to extremely rare changes. *Radiographics*. 2011;**31**:377–390.
- 10) Mori K, Fukuda K, Asaoka H, *et al*. Radiofrequency ablation of the liver: determination of ablative margin at MR imaging with impaired clearance of ferucarbotran-feasibility study. *Radiology*. 2009;**251**:557–565.
- 11) Yoon JH, Lee EJ, Cha SS, *et al*. Comparison of gadoteric acid-enhanced MR imaging versus four-phase multidetector row computed tomography in assessing tumor regression after radiofrequency ablation in subjects with hepatocellular carcinomas. *J Vasc Interv Radiol*. 2010;**21**:348–356.
- 12) Koda M, Tokunaga S, Okamoto T, *et al*. Clinical usefulness of the ablative margin assessed by magnetic resonance imaging with Gd-EOB-DTPA for radiofrequency ablation of hepatocellular carcinoma. *J Hepatol*. 2015;**63**:1360–1367.
- 13) Onishi H, Matsushita M, Murakami T, *et al*. MR appearances of radiofrequency thermal ablation region: histopathologic correlation with dog liver models and an autopsy case. *Acad Radiol*. 2004;**11**:1180–1189.
- 14) Khankan AA, Murakami T, Onishi H, *et al*. Hepatocellular carcinoma treated with radiofrequency ablation: an early evaluation with magnetic resonance imaging. *J Magn Reson Imaging*. 2008;**27**:546–551.
- 15) Kim SM, Shin SS, Lee BC, *et al*. Imaging evaluation of ablative margin and index tumor immediately after radiofrequency ablation for hepatocellular carcinoma: comparison between multidetector-row CT and MR imaging. *Abdom Radiol (NY)*. 2017;**42**:2527–2537.
- 16) Koda M, Tokunaga S, Miyoshi K, *et al*. Assessment of ablative margin by unenhanced magnetic resonance imaging after radiofrequency ablation for hepatocellular carcinoma. *Eur J Radiol*. 2012;**81**:2730–2736.
- 17) Takeyama N, Vidhyarkorn S, Chung DJ, *et al*. Does hepatobiliary phase sequence qualitatively outperform unenhanced T1-weighted imaging in assessment of the ablation margin 24 hours after thermal ablation of hepatocel-

- lular carcinomas? *Abdom Radiol (NY)*. 2016;**41**:1942-1955.
- 18) Sakakibara M, Ohkawa K, Katayama K, *et al*. Three-dimensional registration of images obtained before and after radiofrequency ablation of hepatocellular carcinoma to assess treatment adequacy. *AJR*. 2014;**202**:W487-W495.
 - 19) Makino Y, Imai Y, Igura T, *et al*. Comparative evaluation of three-dimensional Gd-EOB-DTPA-enhanced MR fusion imaging with CT fusion imaging in the assessment of treatment effect of radiofrequency ablation of hepatocellular carcinoma. *Abdom Imaging*. 2015;**40**:102-111.
 - 20) Takeyama N, Mizobuchi N, Sakaki M, *et al*. Evaluation of hepatocellular carcinoma ablative margins using fused pre- and post-ablation hepatobiliary phase images. *Abdom Radiol (NY)*. 2019;**44**:923-935.
 - 21) Boas FE, Do B, Louie JD, *et al*. Optimal imaging surveillance schedules after liver-directed therapy for hepatocellular carcinoma. *J Vasc Interv Radiol*. 2015;**26**:69-73.
 - 22) The Japan Society of Hepatology. Clinical practice guidelines for hepatocellular carcinoma 2013. (accessed 2019 Jun 19) Available from: http://www.jsh.or.jp/English/guidelines_en/Guidelines_for_hepatocellular_carcinoma_2013
 - 23) Kubo M, Matsui O, Sakamoto M, *et al*. Role of gadolinium-ethoxybenzyl-diethylenetriamine pentaacetic acid-enhanced magnetic resonance imaging in the management of hepatocellular carcinoma: consensus at the Symposium of the 48th Annual Meeting of the Liver Cancer Study Group of Japan. *Oncology*. 2013;**84**:21-27.
 - 24) Chinnaratha, MA, Sathananthan D, Pateria P, *et al*. High local recurrence of early-stage hepatocellular carcinoma after percutaneous thermal ablation in routine clinical practice. *Eur J Gastroenterol Hepatol*. 2015;**27**:349-354.
 - 25) Koda M, Tokunaga S, Miyoshi K, *et al*. Ablative margin states by magnetic resonance imaging with ferucarbotran in radiofrequency ablation for hepatocellular carcinoma can predict local tumor progression. *J Gastroenterol*. 2013;**48**:1283-1292.
 - 26) Lee SR, Kilcoyne A, Kambadakone A, *et al*. Interventional oncology: pictorial review of post-ablation imaging of liver and renal tumor. *Abdom Radiol (NY)*. 2016;**41**:677-705.
 - 27) Sotirchos VS, Petrovic LM, Gonen M, *et al*. Colorectal cancer liver metastases: biopsy of the ablation zone and margins can be used to predict oncologic outcome. *Radiology*. 2016;**280**:949-959.
 - 28) Vandembroucke F, Vandembroucke J, Buls N, *et al*. Can tumor coverage evaluated 24 h post-radiofrequency ablation predict local tumor progression of liver metastases? *Int J Comput Assist Radiol Surg*. 2018;**13**:1981-1989.

[Received June 20, 2019 : Accepted August 2, 2019]